Chemical Geology 360–361 (2013) 241–251

Contents lists available at ScienceDirect

Chemical Geology

journal homepage: www.elsevier.com/locate/chemgeo

Tracing euxinia by molybdenum concentrations in sediments using handheld X-ray fluorescence spectroscopy (HHXRF)

Tais W. Dahl [a,b,*], Micha Ruhl [b,c], Emma U. Hammarlund [a], Donald E. Canfield [a], Minik T. Rosing [b], Christian J. Bjerrum [c]

[a] Nordic Center for Earth Evolution and University of Southern Denmark, Campusvej 55, DK-5230 Odense M, Denmark
[b] Nordic Center for Earth Evolution (NordCEE), Natural History Museum of Denmark, University of Copenhagen, Øster Voldgade 5-7, DK-1350 Copenhagen K, Denmark
[c] Nordic Center for Earth Evolution (NordCEE) and Department of Geosciences and Natural Resource Management, University of Copenhagen, Øster Voldgade 10, DK-1350 Copenhagen K, Denmark

ARTICLE INFO

Article history:
Received 14 August 2012
Received in revised form 18 October 2013
Accepted 20 October 2013
Available online 31 October 2013

Editor: Michael E. Böttcher

Keywords:
Molybdenum
Paleo-redox
Black shales
Anoxic environments
Handheld
XRF

ABSTRACT

Elevated molybdenum (Mo) contents in organic-rich sediments are indicative of deposition from an anoxic and sulfide-rich (euxinic) water-column. This can be used for tracing past euxinic conditions in ancient oceans from sedimentary archives. Conventional analytical detection of elevated molybdenum levels is, however, expensive and cannot be directly performed in the field. Here, we show that handheld x-ray absorption spectroscopy (HHXRF) on both rock-powders and rock surfaces provides a powerful tool for laboratory or field-based, geochemical characterization of Mo content and the tracing of euxinic depositional conditions. We further present a sedimentary Mo database, compiled from over 300 globally distributed modern marine sites, to show that modern euxinic marine basins are characterized by molybdenum enrichment (>25 ppm) relative to average crust (~1.5 ppm) and river suspended matter (~3 ppm). Only Mn-oxide rich deposits from oxygenated deep sea settings match such high Mo enrichments, but these are easily distinguished from Mo-rich sediments from the continental shelves. Hence, past and present organic rich sediments enriched in Mo are indicative of (at least intermittent) water-column euxinia.

We analyzed the molybdenum content of powdered and homogenized samples of Holocene, Miocene, Triassic–Jurassic, Ordovician and Cambrian age by HHXRF and Inductively-Coupled-Plasma-Mass-Spectrometry (ICPMS). We further analyzed 2 certified NIST standard references (NIST-2781 with Mo: 47 ppm and NIST-2702 with Mo: 10 ppm) for analytical control. Analytical precision (1σ) after 30, 120, and 300 seconds of measuring time was 4, 2, and 1 ppm, with a respective detection limit of 11, 5, 3 ppm (3σ, noise level). The data were accurate to within the given precision (1σ) after a daily calibration to samples covering a range of Mo concentrations from 0 to >30 ppm.

Hand-held XRF equipment also allows Mo measurements directly on fresh rock surfaces, both in the field and under laboratory conditions. Rock-samples from a Cambrian drill core closely match ICPMS obtained Mo concentrations from homogenous powders of the same rocks. Collectively, our data show that HHXRF as a quick and reliable method for the precise and accurate quantification of molybdenum concentrations in both rock powders and at fresh rock surfaces. The non-destructive nature of the HHXRF measurements is combined with low (per sample) analytical costs, minor sample preparation and easy applicability in the field.

1. Introduction

Wilhelm Roentgen discovered X-rays in 1895, and elemental spectra, forming the basis for X-Ray fluorescence, were identified and quantified in 1913 by Henry Moseley (Moseley, 1913). The first commercial XRF spectrometers became available in the 1950s and were greatly improved after the development of solid-state detectors in the 1960s. XRF spectrometry is often applied in geochemical studies to determine concentrations of major elements (with >wt.% abundance) and some trace elements, but the instruments are expensive. Handheld-XRF (HHXRF) spectrometers are now commercially available, and can be brought into the field for easy use. This paper aims to determine the applicability of HHXRF for studying Mo concentrations in sediments and sedimentary rocks, which finds important applications in economic geology and paleo-environmental studies. We test the method by studying sediments with varying Mo concentrations and compare HHXRF with ICPMS measurements.

Current understanding of the evolution of ocean chemistry implies fully anoxic conditions throughout the Archean Eon (>2500 Ma), developing into anoxic deep waters and oxygenated surface waters in the Proterozoic Eon (2500–542 Ma) and a massive, but protracted, rise of O_2 from the Neoproterozoic Eon (1000–542 Ma) into the Paleozoic Era (542–251 Ma) (Holland, 1984; Farquhar et al., 2000; Poulton et al., 2004; Canfield, 2005; Holland, 2006; Scott et al., 2008; Dahl

* Corresponding author.

0009-2541/$ – see front matter © 2013 Elsevier B.V. All rights reserved.
http://dx.doi.org/10.1016/j.chemgeo.2013.10.022

et al., 2010b). Ocean anoxic events are known to have occurred throughout the Phanerozoic (e.g., Schlanger and Jenkyns, 1976; Knoll et al., 1996; Isozaki, 1997; Meyer and Kump, 2008; Jenkyns, 2010; Gill et al., 2011; Hammarlund et al., 2012). Today, anoxic and sulfidic waters are relatively rare; restricted basins with slow water circulation such as the Black Sea, the Cariaco Basin, the deepest parts of the Baltic Sea and several, globally distributed, fjords contain anoxic bottom waters with free sulfide (Meyer and Kump, 2008). Further, hydrogen sulfide is present at low level in the upwelling zone offshore Peru and accumulates seasonally in the anoxic marine upwelling zones such as Walvis bay, offshore Namibia, and along the Peruvian margin (Lavik et al., 2009). Free sulfide (S^{2-}, HS^- and H_2S) accumulates in anoxic waters, where the rate of microbial sulfate reduction outpaces the supply of Fe^{2+} to the aquatic reservoir. Anoxic and sulfidic water-column conditions are termed 'euxinic' and sediments deposited under these conditions constitute major sinks for a range of transition metals (including molybdenum), both in modern and ancient oceans (Calvert and Pedersen, 1993; Lyons et al., 2009).

The availability of O_2 and H_2S in the water column is a key factor dictating the geochemical behavior of Mo (e.g., Helz et al., 1996; Anbar, 2004). In oxic depositional environments, Mo exists as soluble molybdate (MoO_4^{2-}) that adsorbs onto Mn-oxides via polynuclear species (i.e. hexamolybdate, Wasylenki et al., 2011) and only slowly precipitates in the modern ocean (Bertine and Turekian, 1973; Scott et al., 2008). In sulfidic waters, Mo-sulfide precipitates out of solution, leading to strong sedimentary Mo enrichments (S. Emerson and Huested, 1991; Helz et al., 1996). The activity of sulfide plays a critical role in the removal process, plausibly due to the activation energy needed for breaking the strong Mo═O bonds in MoO_4^{2-} to form thiomolybdate anions with softer sulfur ligands ($MoO_{4-x}S_x^{2-}$). Tri-thiomolybdate is rapidly reduced to highly reactive Mo(IV)-sulfides (Vorlicek et al., 2004; Dahl et al., 2013). The Mo(IV)-sulfides are readily scavenged with Fe-sulfides and perhaps sulfur-rich organic molecules, and there is a close correlation between Mo and total organic carbon content (S. Emerson and Huested, 1991; Huerta-Diaz and Morse, 1992; Vorlicek and Helz, 2002; Bostick et al., 2003; Helz et al., 2004; Tribovillard et al., 2004; Vorlicek et al., 2004; Algeo and Lyons, 2006; Helz et al., 2011). Importantly, thiomolybdate formation appears to be the rate-limiting step in the removal process and requires significant levels of aqueous H_2S (Erickson and Helz, 2000; Vorlicek et al., 2004; Dahl et al., 2013). At a pH of 7–8 and temperatures of 4–25 °C, this threshold is passed at total sulfide levels of 15–125 μM (Hershey et al., 1988). This relatively high sulfide activation level is required to initiate the Mo enrichment process in euxinic sediments compared to, for example, FeS and pyrite formation (Dahl et al., 2011). In addition to the H_2S requirement to form thiomolybdates at low pH, FeS preferentially forms at high pH since it requires S^{2-} to form FeS from Fe^{2+}. Thus, efficient Mo scavenging is predicted to occur at a narrow pH-range around 7, where both sulfide species coexist (Helz et al., 2011).

Recently, Scott and Lyons compared sediments deposited in euxinic and non-euxinic settings, where sulfide is sometimes present, yet always restricted to the pore fluids. They proposed that sedimentary Mo contents greater than 25 ppm is a characteristic signature of sediment deposition under a euxinic water column in todays oceans (Scott and Lyons, 2012). Here, we apply handheld XRF to a wide range of modern sediments and ancient sedimentary rock archives to show in Section 4 that the sedimentary Mo content is reliably determined well below 25 ppm and that the method also works for fresh rock-surface analysis. Then in Section 5, we compare the sedimentary Mo-contents database that now includes more than 300 modern marine sites to a broad range of redox environments. This confirms >25 ppm sedimentary Mo as useful marker for characterizing euxinic deposition today. Finally, we discuss how this can be used for recognizing euxinic depositional environments throughout Earth's past, and we highlight the advantages of using Mo and HHXRF in comparison to other redox proxies.

2. Materials

Five sedimentary sequences of Holocene, Miocene, Triassic–Jurassic, Ordovician and Cambrian age were analyzed to test how reliable handheld X-Ray-Fluorescence identifies organic-rich sediments with >25 ppm Mo, indicative of deposition under euxinic water-column conditions.

- Holocene sediment samples were taken from a 9-meter long core drilled through permanently euxinic Lake Cadagno, Switzerland (46°33′01″N, 008°42′41″E). The core was retrieved during a field campaign in 2009. Samples were radiometrically dated and represent ~9800 yrs of euxinic deposition (Wirth et al., 2013). The mostly silty sediments contained several wt% organic carbon. Sedimentological and biogeochemical description is reported in (Wirth et al., 2013). HHXRF measurements were performed on bulk (powdered) sediments showing Mo concentrations ranging from 3 to 200 ppm, with the low concentrations found in association with turbiditic influx of oxic sediments from the shallow basin margin.
- Late Cambrian (uppermost Mid Cambrian–Furongian, ~500 million year old) sedimentary rocks from the Alum shale formation were sampled from the Andrarum-3 drill-core SE Scania, Sweden (55°42′ 55.75″N, 013°58′41.25″E). The samples are black-shales originating from a marine depositional environment (Ahlberg et al., 2009). HHXRF analyses were performed both directly on fresh rock surfaces without any further sample preparation and on bulk powders, crushed with a jaw crusher and agate mortar. The Andrarum-3 sediments contain ~10 wt.% organic carbon, and redox sensitive metals suggest a euxinic depositional environment (Dahl et al., 2010b; Gill et al., 2011). However, the presence of benthic trilobites at several horizons suggests, at least, intermittently oxygenated bottom-water conditions (Lauridsen and Nielsen, 2005). Sedimentary geochemistry shows strong enrichments of highly reactive iron relative to total Fe ($Fe_{HR}/Fe_T > 0.38$), indicative of Fe^{2+} transport in anoxic basinal bottom waters and with a large proportion of the highly reactive Fe retained as pyrite ($Fe_{PY}/Fe_{HR} > 0.8$). These parameters form an independent confirmation of euxinic conditions in the depositional environment (e.g., >7 μM total sulfide). Mo concentrations measured by quadrupole ICPMS range from 3 to 125 ppm (Dahl et al., 2010b; Gill et al., 2011).
- Triassic–Jurassic (uppermost Rheatian–Hettangian, ~201 million years old) sediments were sampled at St. Audrie's bay (51°10′54.70″ N, 003°17′09.79″W) and East Quantoxhead (51°11′27.91″N, 003°14′ 12.25″W), southwest UK. The sediments were deposited in a marginal marine basin. The precession-paced deposition of laminated black-shales alternates with gray muds (Ruhl et al., 2009). Total organic carbon contents range up to 12 wt.% (Ruhl et al., 2009). Sedimentary Mo concentrations were measured both by HHXRF on agate-mortar powdered samples and ICPMS at the Geological Survey of Greenland and Denmark (GEUS, methods described in Hammarlund et al., 2012). The Mo_{ICPMS} contents range from 2 ppm in gray mudstone sediments to 212 ppm in the laminated black shale sediments. In general black shales have Mo > 25 ppm associated with high concentrations of isorenieratane (Jaraula et al., 2013) and Fe_{HR} / $Fe_T > 0.38$, Fe_{PY} / $Fe_{HR} > 0.5$ (Ruhl et al., in prep.).
- Ordovician–Silurian (Hirnantian–Rhuddanian, ~440 million years old) samples come from both the Upper Hartfell and the lower Birkhill shale of the Moffat shale group at Dob's Linn, Southern Uplands, Scotland (55°25′47.56″N, 003°16′72.91″W), and from the Billegrav-2 drill core through the Lindegård formation and the Rastrites shales, Bornholm, Denmark (55°00′44.64″N, 014°59′54.42″E). The sediments at Dobs Linn were deposited in a deep-water setting during late Hirnantian glaciation and two contemporaneous biotic extinction events. The sediments were deposited from oxic waters during the glaciation, which ended with transgression resulting in the deposition of black shales with <2 wt.% organic carbon and high pyritic iron

fraction ($Fe_{HR}/Fe_T > 0.38$, $Fe_{PY}/Fe_{HR} > 0.7$) indicative of euxinic deposition (Hammarlund et al., 2012). Mo concentrations obtained with ICPMS at Arizona State University range from 2 to 41 ppm (Dahl et al., 2010b). The Rastrites shales at Billegrav-2 span gray to black mudstones recording Fe speciation signatures with both oxic and anoxic euxinic signatures. Mo concentrations from 0.2 to 39 ppm are observed in the sequence with the highest concentrations coinciding with euxinic Fe speciation signature (Hammarlund et al., 2012).

- Miocene sediment samples were taken from cores on the New Jersey Shelf at 204 to 354 mbsf and 558 to 673 mbsf (Site 27A and 29A at 36°38.04606′N, 73°37.30146′W, water depth: 33.5 m and 39°31.1705′N, 24.7925′W, water depth: 35.97 m, respectively). The cores were retrieved as part of IODP Expedition 313 and dated by biostratigraphic and chemostratigraphic methods (Mountain et al., 2010). The mostly silty mud sediments contained between 1 and 6 wt% organic carbon, where atomic C/N ratios of ~20 indicate that approximately 30% is of marine origin (Fang et al., 2013). Sedimentary geochemical analyses shows strong enrichments of highly reactive iron relative to total Fe ($Fe_{HR}/Fe_T > 0.38$), with highly reactive Fe retained as pyrite ($Fe_{PY}/Fe_{HR} \sim 0.7$) where Mo > 10 ppm (Bjerrum et al., in prep.). Prevailing bioturbation and only few laminated and non-bioturbated horizons together with Fe speciation data, suggest intermittently anoxic bottom-water conditions in a predominantly oxygenated shelf setting. Sedimentary Mo concentrations were measured both by HHXRF on agate-mortar powdered samples and by ICPMS at the Geological Survey of Denmark and Greenland (GEUS, methods described in Hammarlund et al., 2012). Mo_{ICPMS} contents range from 1.0 to 20 ppm.

3. Methods

3.1. Hand-held X-ray fluorescence (HHXRF)

Mo concentrations in powders and on rock surfaces were quantified using a handheld energy dispersive XRF spectrometer (EDXRF) alpha-8000 LZX from Innov-X/Olympus. The instrument contains a battery operated miniature X-Ray source (W anode) and no radioisotopes, hence it requires no special licensing during international transportation. The instrument was either held in hand (for rock surfaces) or installed in a stand (for powders). The X-ray beam covers an area of ~2 cm^2 (1.5 × 1.3 cm) at the port. X-ray absorption spectra were recorded in scanning mode from 3 to 40 keV and absorption peaks were automatically identified using the Innov-X "soil mode" software. The software determines Mo at the Ka edge at 17,479.3 eV where no correction is needed for elemental interferences. The signal is automatically corrected for Compton noise recorded at several energy levels outside elemental absorption peaks. The Compton normalization (background noise correction) is matrix dependent and was calibrated for solid surfaces and powder samples. Powders were measured directly in their containers by covering the opening with a thin layer of kitchen wrap. Thin kitchen wrap was transparent at the Mo Kα line, but thicker plastics (transparencies and plastic pockets) would compromise the absorption signal. Thin layers of powder (<3 mm) suffered from improper Compton normalization yielding a positive Mo offset (Fig. 1). Therefore, HHXRF analysis was performed either on rock surfaces or on >4 mm thick layer of powder. We did not observe any signal loss between flat and imbricate surfaces, unless the field of view was not entirely covered. Conversion from absorption to concentrations was performed after calibration at the stainless steel target and subsequent data reduction was performed with Innov-X soil software that included a five-point calibration curve with 1.6–46.7 ppm Mo NIST standards (NIST 2702, NIST 2709, NIST 2710, NIST 2711, NIST 2781).

The analytical precision of handheld XRF analyses improves with increased counting time; 1σ error on the counting statistics was ±4, ±2 and ±1 ppm for 30, 120 and 300 seconds of analysis on NIST 2781, respectively. The detection limit is reported as 3 times the standard error of the blank level (3σ), typically 11, 15, and 3 ppm, respectively. The level of quantification is traditionally defined at 10σ (>10 ppm). In most cases, even 30 seconds is sufficient for general field measurements, while 60 s is recommended for more accurate analyses between 20 and 30 ppm. Longer exposure time is favored in the laboratory, where the HHXRF can be placed in a stand.

A wide range of elements heavier than Na is automatically detected and quantified during HHXRF analysis, including Ba, V, Cr, Ni, Cu, Zn, Rb, Sr, Y, Zr, Nb, Mo, Th, and U (Rowe et al., 2012).

Several lighter elements are harder to quantify due to atomic interferences in the x-ray absorption spectrum. Typically, Al or Ti has been used to normalize Mo enrichments in sediments relative to clay contents. Indeed, this would highlight samples with substantial proportion of detrital components, such as biogenic carbonate and/or quartz. Contrary, it may devalue organic-rich samples, since Mo is hosted with (sulfurized) organic matter and/or Fe-sulfide minerals in euxinic sediments (decoupled from Al or Ti). Thus, because Mo contents in crustal materials (~1 ppm) and (non-sulfurized) particulate organic matter (<5 ppm) are low, the

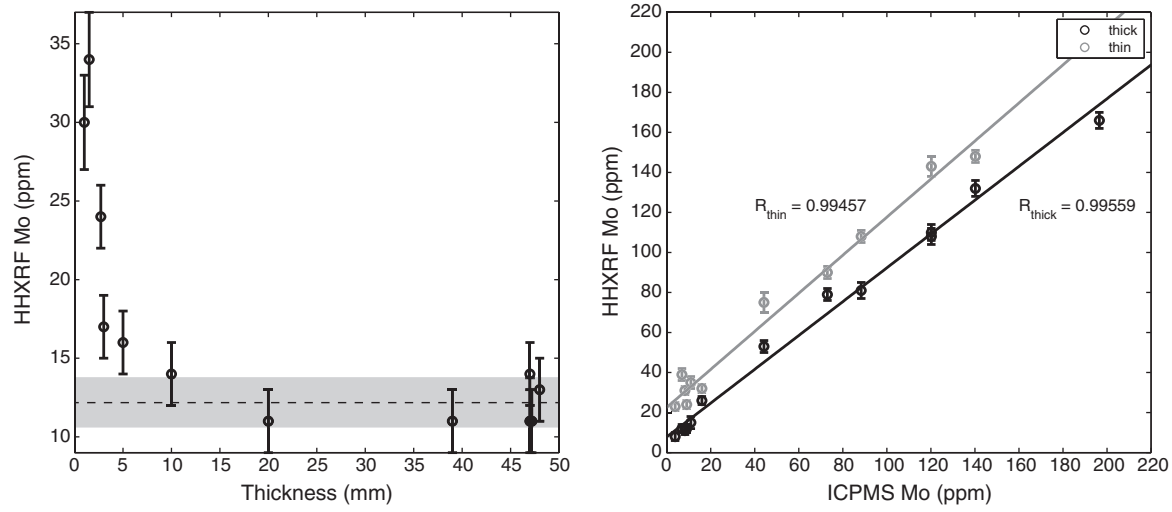

Fig. 1. a) Mo concentration in a silt sample-powder measured at variable thickness of the powder layer. The mean value and 1 standard deviation of the mean are shown in light color for the sample measured at a thickness of 47 mm (12.3 ± 1.5 ppm, n = 3). b) Mo concentrations measured using HHXRF versus ICPMS data for 1 mm thin (gray) and >4 mm thick samples (black). The HHXRF Mo concentration data is linearly correlated to the ICPMS data with Pearson correlation coefficients R^2 >0.99 for both thin and thick target powders.

detrital dilution will only lower the observed sedimentary Mo content, and thus never produce false identification of modern or past ocean euxinia (i.e. >25 ppm). Our database of sedimentary Mo contents in modern-day marine environments shows that normalization (e.g. against Al or Ti) is unnecessary for reliable identification of euxinic ocean conditions (Section 5.1).

3.2. Inductively coupled plasma mass spectrometry (ICPMS)

For comparison, sedimentary Mo contents were also measured with ICPMS. The analyses of Triassic–Jurassic, Ordovician and Miocene samples were performed at the Geological Survey of Denmark and Greenland (GEUS) as described in Hammarlund et al. (2012).

Cambrian samples were measured at Arizona State University (Dahl et al., 2010b). The Holocene samples from Lake Cadagno were measured in Langmuir Lab at Harvard University using the following (similar) method. Samples were first dried, then ashed at 900 °C, and crushed by mortar and pestle. The powders were dissolved using the PicoTrace digestion system with two digestion steps. Ashed powders were loaded into Teflon beakers with concentrated HF + HNO_3 in a 3:1 ratio, sealed, and installed on a heating block. They were left at 110 °C for 48 h, then, dried down and re-dissolved in 6 M HCl during another heating cycle. Finally, samples were dried down and re-dissolved in 5% HNO_3 before quantification using a Thermo Scientific X-Series q-ICPMS. The analytical precision was better than 1% on the same solution (1 s.d. = standard deviation, sample reproducibility). Accuracy was estimated from measurements of two certified USGS standards (SCO-1 and BCR-2). Mo-contents were determined at 1.10 ppm and 286 ppm (with <1% reproducibility) which is -1.5 s.d. and +2.2 s.d. from the certified mean values at 1.4 ± 0.2 ppm and 248 ± 17 ppm (mean ± s.d., precision), respectively.

4. Results and discussion

4.1. Comparison of HHXRF and ICPMS data

Raw Mo concentration data are shown in Fig. 2 and tabulated in Table S1. Data obtained with HHXRF and ICPMS correlate well in all analytical session with Pearson correlation coefficients $R^2 > 0.9$ for sample sets spanning more than 30 ppm Mo in range (Table 1). Remarkably, the conversion from counts-to-concentration is acceptable after measuring only one calibration target of stainless steel (16,200 ppm Mo), which greatly simplifies HHXRF identification of samples with >25 ppm Mo. As shown below, this means euxinic characterization can be made in the field with no need for further re-calibration.

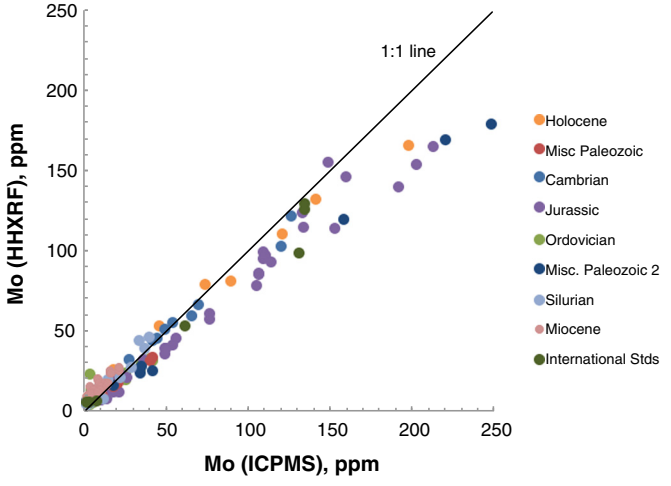

Fig. 2. Raw HHXRF Mo concentration determinations vs. ICPMS data for n = 82 samples (no daily matrix-matched re-calibration). Two outliers were discarded (marked in *italic* in Table S1). Tabulated data are provided in Table S1.

The slope (a) and intercept (b) of the linear correlation relationships were determined on nine different samples sets, $Mo_{HHXRF} = a \cdot Mo_{ICPMS} + b$ and fitting results were summarized in Table 1. We find slopes that are systematically lower than unity (a = 0.85 ± 0.10, 1 s.d.) and positive intercepts (b = 5 ± 3 ppm, 1 s.d.) (Table 1). The slope varied from unity by −27% to +15% and the intercept was positively offset at b = 4 ± 3 ppm in all sessions. Hence, a sample with only ~2 ppm Mo would yield 2 + b = 6 ± 3 ppm using HHXRF, and highly concentrated samples would display concentrations ~20% lower than the actual content. Hence, the here used HHXRF-system displays too high readings for the lowest Mo contents (<20 ppm) and too low readings for the most enriched samples.

Because, this relationship is systematic, it can be corrected for by re-calibration to certified (or calibrated lab-) standards. The corrected HHXRF data was offset <13% in eight certified reference materials with Mo contents up to 248 ppm. The Innov-X software allows for a permanent re-calibration with an extra "fundamental parameters" module so that similar data quality could be obtained in the field.

The reproducibility of a sample over different days of operation is exceptional, no matter measurement conditions. For example, NIST 2781 and NIST 2702 were found at 37 ± 1 ppm (1 s.d., n = 9 sessions, certified 46.7 ± 3.2 ppm) and 15 ± 1 ppm (1 s.d., n = 7, certified 10.8 ± 1.6 ppm Mo), respectively. A linear correction ($Mo_{HHXRF} = a \cdot Mo_{true} + b$; a = 0.63, b = 8.2) would produce the correct NIST calibration. Hence, a linear correction based on the average of the samples and other standards (a ≈ 0.8, b ≈ 4, Table 1) would generally also improve the accuracy of the measured NIST standards. The linear offset is not explained by daily drift or change of instrumental settings in the HHXRF spectrometer, but may result from matrix-dependency in the calibration standards (e.g. physical and chemical properties of the analyzed material). The accuracy of the HHXRF was evaluated using eight certified standards with 0.4–248 ppm Mo (Session 9: SCO-1, JDO-1, ZGI-TS, ASK-1, MAG-1, FC-1, SDO-1, BCR-2). The corrected data falls within 1 s.d. (<13%) of the certified values (Table 2). The corrected data carry larger error due to error propagation from a and b, and are in good agreement with certified values for eight reference materials. In a handful of samples, we have seen that our ICPMS data are severely underestimated, which we ascribe to either spill or incomplete dissolution during sample preparation for the mass spectrometric analysis (Table S1).

HHXRF data from Lake Cadagno sediments was compared to published results from Core Scanning XRF (CSXRF), at 1 mm stratigraphic resolution on a separate core (Wirth et al., 2013). Different recording of stratigraphic variability in Mo contents between both HHXRF and ICPMS falls, falls within the sedimentary Mo range observed using CSXRF in the sample intervals (Fig. 3).

We recommend that HHXRF analysts include a set of reference materials (samples with independent Mo constraints) spanning more than 30 ppm Mo from the level of detection to well above the 25 ppm Mo threshold. Preferably, one should use calibration standards with similar physical and chemical properties (e.g. powder grain size and lithology) instead of the default calibration based on fine-grained and compressed NIST powders. The reported data should be presented together with precision and accuracy of reference materials.

4.2. HHXRF on rock surfaces

Mo concentrations were also determined directly on the bedding planes of unpolished rock surfaces and compared to bulk rock ICPMS data from the Andrarum-3 drill core (Fig. 4). The HHXRF data (n = 107) was obtained in 8 h (30 s per analysis) whereas our ICPMS data (n = 50) was collected over several weeks of labor-intensive sample preparation with acid digestion and costly analysis. The HHXRF Mo record tightly follows the ICPMS Mo record showing the main features

Table 1
Linear fitting results for the Mo data obtained with HHXRF and ICPMS, where $Mo_{HHXRF} = a. Mo_{ICPMS} + b$, n and R are the number of samples and Pearson correlation coefficient, respectively.

Session		Samples within the NIST calibration					Extrapolation to full Mo range in sample set				
#	Sample set	Range (ppm)	a	b	R^2	n	Range (ppm)	a	b	R^2	n
1	Lake Cadagno	7–44	1.15 ± 0.08	3.2 ± 1.6	0.979	6	4–197	0.85 ± 0.02	7.8 ± 2.0	0.991	12
2	Chengjiang, Dob's Linn	10–41	0.73 ± 0.02	2.7 ± 0.4	0.999	5					
3	Andrarum-3	18–48	1.04 ± 0.11	1.1 ± 4.2	0.966	5	3–125	0.85 ± 0.03	7.7 ± 1.9	0.988	12
4	Triassic–Jurassic	8–35	0.81 ± 0.08	1.7 ± 1.5	0.853	18	2–212	0.81 ± 0.02	2.6 ± 1.6	0.977	48
5	Dob's Linn	8–41	0.70 ± 0.04	4.7 ± 1.0	0.946	17	2–41	0.74 ± 0.03	4.7 ± 1.0	0.964	22
6	Misc. Paleozoic	17–41	0.45 ± 0.19	9.1 ± 6.0	0.758	4	0.7–248	0.73 ± 0.01	3.4 ± 1.4	0.997	12
7	Billegrav-2	6–39	1.09 ± 0.08	2.4 ± 1.6	0.937	14	0.2–39	1.06 ± 0.04	3.2 ± 0.6	0.950	31
8	Miocene	6–20	0.91 ± 0.17	8.2 ± 2.0	0.659	17	0–20	0.88 ± 0.07	8.6 ± 0.6	0.810	38
9	Int. standards						6–134	0.85 ± 0.08	0.6 ± 6.6	0.966	6

of the Mo profile. Yet, a few samples showed different Mo contents when comparing surface rocks and powdered rock. Whole-rock HHXRF measurement was performed on the bedding-plane of the host-rock and thus integrates Mo content only over ~30 μm stratigraphic thickness, while ICPMS measurement of powders integrates over the full stratigraphic thickness of the powdered sample. Supporting this, spatial heterogeneity in Mo concentrations was found between two adjacent bedding-plane measurements using the HHXRF to the surface ~1 cm apart (Fig. 4). Similar variability occurs in the Holocene CSXRF data set from Lake Cadagno sediments (Fig. 3). Traditional sampling for ICPMS would crush and homogenize a rock of comparable thickness and thus obscure local Mo variability. Indeed, most bedding planes ~1 cm apart showed remarkably little Mo variability, but subtle variations could be observed at specific stratigraphic intervals (Fig. 4). In more than 75% of the analyzed samples (n = 107) bedding planes ~1 cm apart deviated from their mean value by less than 22%. Large deviations from mean of greater than 50% and 100% magnitude were observed in only 17 and 4 samples, respectively. For example, HHXRF recorded different sedimentary Mo contents of 16 & 111 ppm and 18 & 90, on the sediment bedding-planes at 9.37 & 9.38 m and 24.04 & 24.05 m, respectively (Fig. 4).

Sudden decrease in Mo contents in sediments formed under presumably euxinic settings is potentially caused by: 1) Turbiditic dilution with Mo-lean material, 2) oxidative dissolution of Mo-sulfides (e.g., in outcrop samples), 3) rapid redox change in the local depositional environment, such as during periods with oxygenated bottom waters associated with changes in primary productivity or water circulation. With HHXRF one can perform high-resolution Mo profiling that may assist the sedimentologist in identifying periods of persistent euxinia that can promote further investigation by thin section petrography, laser ablation ICPMS, or other refined methods (Macquaker et al., 2010).

Table 2
Mo data from reference materials obtained using handheld XRF are shown with their certified Mo contents. Raw data and corrected data are shown. Errors represent 1σ-propagated uncertainty from linear correction and counting statistics. All data and session are tabulated in Table S1.

Name	Material	Mo (ppm)	Raw HHXRF	Corrected HHXRF
SCo-1	Cody Shale, USGS	1.4 ± 0.2	<5	<5
JDO-1	Dolomite, Geol. Surv. Japan	0.27–0.40	<5	<5
ZGI-TS	Black shale, CMEA[b]	130 ± ?	98 ± 2	115 ± 10
ASK-2	Schist powder[b]	60	53 ± 2	62 ± 8
MAG-1	Marine Sediment, USGS	1.6	<5	<5
FC-1	Fish Clay 1, IAG[a]	6.2 ± 0.85	6 ± 2	6 ± 7
SDO-1	Ohio Shale, USGS	134 ± 21[c]	129 ± 3	151 ± 13
−*rpt*	–	134 ± 21	126 ± 2	148 ± 12
BCR2	Columbia River Basalt, USGS	248 ± 17	179 ± 5	241 ± 4

[a] Mao et al., 2001.
[b] Govindaraju, 1994.
[c] Schnetger (1997) determined the Mo content in SDO-1 using four distinct methods 161 ppm (XRF), 155 ppm (AAS), 147 ppm (ICP-OES) and 146 ppm (ICPMS), all suggesting the certified average value is too low (Schnetger, 1997).

5. Tracing euxinic conditions from sedimentary Mo content

5.1. Sedimentary Mo database from modern marine settings

To date, sedimentary Mo concentration profiles have been reported for more than 300 marine localities worldwide spanning the range of redox conditions in modern environments (Fig. 5). Elevated sedimentary Mo contents are often considered characteristic of deposition under sulfidic water-column condition (Calvert and Pedersen, 1993; Lyons et al., 2009), but the Mo database has not been systematically investigated with respect to redox compositions of the water column and sediment in which Mo was deposited. Therefore, we have compiled this comprehensive data set for modern marine redox-environments to evaluate whether elevated Mo concentrations is an adequate indicator of water-column euxinia (Table S2). For 136 sediment cores, O_2 and H_2S concentrations in the water-column and in the underlying sediments were reported (Fig. 6), and redox conditions could be inferred from other reports in another 172 cores (Figs. 5, 6a–b). The redox settings were subdivided into seven groups depending on whether O_2 or H_2S was present in the water column and/or sediments. We define $O_2 > 10$ μM in the bottom waters as oxic conditions, because Mn-oxides are known to persist in the sediment at this or higher O_2 levels (Shaw et al., 1990). Euxinic conditions were defined based on >10 μM aqueous H_2S_{aq} where molybdate is thiolated to form reactive thiomolybdate (Erickson and Helz, 2000; Vorlicek et al., 2004; Dahl et al., 2013). An overview of the studied sections is summarized in Table 1. This redox-assigned Mo database (Figs. 5 and 6, Tables 3 and S2) leads to a similar conclusion as a recent study of only a subset of the reported sites in the database (Scott and Lyons, 2012).

Sediments in all modern-day marine euxinic environments show strong >10-fold Mo enrichment relative to average upper continental crustal value (Fig. 6). We find that a minimum of >25 ppm Mo in marine sediments includes almost all modern euxinic depositional environments, consistent with (Scott and Lyons, 2012). Two sites from the deep Black Sea, however, contain only 10–12 ppm Mo. Low Mo contents in the marine unit 1 are also found in mudflows deposited in the central part of the Black Sea at 2218 m water depth (Piper and Calvert, 2011). These intervals represent mass flow movement and transport of Mo depleted sediment from the oxic shelf to the deep euxinic basin. Other modern-day marine euxinic sites (n = 31) display strong Mo enrichment.

A critical role for H_2S is expected from laboratory studies and consistent with low concentrations of sedimentary Mo observed in anoxic and non-sulfidic regions of the Arabian Sea and the Baltic Sea (Pattan and Pearce, 2009; Scholz et al., 2013). In other major oxygen minimum zones (e.g. off the coast of Namibia, Peru, and Chile), observed 10–50 ppm sedimentary Mo enrichments, most likely result from episodic availability of H_2S in the water-column, with reported values offshore Namibia of ~10–68 μM total H_2S (Brongersma-Sanders et al., 1980; Böning et al., 2004; Weeks et al., 2004; Lavik et al., 2009; Schunck et al., 2013). Potentially seasonal free sulfide availability in the water-

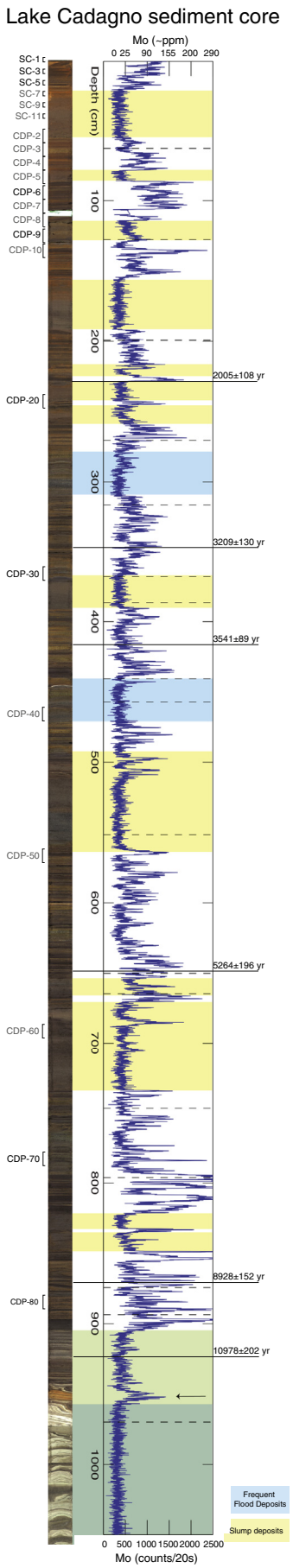

Fig. 3. Stratigraphic view of the HHXRF (◊) and ICPMS (red, ▪) Mo data from Lake Cadagno sediment cores overlain Mo data obtained using core scanning XRF (blue –, CSXRF, Wirth et al., 2013). HHXRF and ICPMS data are obtained from sediment homogenized over the length scale shown, whereas CSXRF is obtained directly from the surface sediment from a separate drill core retrieved very close to the one analyzed with HHXRF and ICPMS. See Wirth et al., 2013 for correlations the two sediment cores. (For interpretation of the references to color in this figure legend, the reader is referred to the web version of this article.)

column in these settings may promote Mo removal, however, the potential link between Mo precipitation and seasonal H_2S availability needs further study.

Molybdenum can be concentrated in oxic sediments by co-precipitation with Mn-oxide solid phases, which are stable in sediments at >10 μM O_2 (Shaw et al., 1990). Severe Mo enrichments (300–700 ppm) can occur under oxic conditions in the deep ocean, into small, rounded manganese nodules mainly containing Fe and Mn-oxides. These extreme Mo concentrations are a result of the exceptionally slow formation rates of the Mn nodules. Mo enrichments of up to 60 ppm can also be found in horizontal deep-sea sediments (>3100 m water-depth, MANOP-sites and off-shore Baja, East Pacific, Shimmield and Price, 1986; Brucker et al., 2009). However, Mo is at these sites re-dissolved by pore fluids as a consequence of reductive dissolution of Mn-oxides that liberates Mo into (weakly) oxygenated pore spaces at 5–30 cm below the sea bed (Bender and Heggie, 1984; Morford and Emerson, 1999; Morford et al., 2005). This process usually leaves little or no Mo enrichment in the deeper sediments. The same behavior is observed on the non-euxinic shelves, but here deposits never exceed 25 ppm Mo. Examples from the shelves with declining Mo concentration as a function of depth include the shallow Baffin Bay (Huerta-Diaz and Morse, 1992) and estuaries at Bay of Biscay, Gulmar Fjord, Loch Etive (Malcolm, 1985; Chaillou et al., 2002; Goldberg et al., 2012). Similar or smaller enrichments occur in oxic sediments with sulfide present only in the sedimentary pore fluids (Zheng and Anderson, 2000). Therefore, these oxic sites define the Mo threshold at 25 ppm with higher enrichments only preserved in modern (intermittently) euxinic shelf sediments.

Our comparative study shows that >25 ppm Mo enrichments in marine sediments occur either in permanently euxinic settings, in intermittently hydrogen sulfide bearing settings. Alternatively, Mo can be enriched at deep-ocean, oxic, abyssal-settings, in association with the formation of Mn oxide nodules or ferromanganese sediments. However, most of the abyssal ocean floor contains little or no authigenic Mo, simply because both O_2 and H_2S are so low that neither Mn-oxides nor hydrogen sulfide accumulate. Sedimentary Mo enrichment through either the oxic or sulfidic removal pathway can easily be distinguished by considering host mineralogy, Mo speciation, and/or geological context. For example, 1) Mo retained in Mn-oxides is simply distinguished from Mo in sulfidic deposits by thin-section or even hand-lens inspection, by the lack of organic matter and sulfides (e.g. pyrite) in the Mn oxide deposits and, of course, the presence of high concentrations of Fe- and Mn-oxides. 2) The Mo-oxide phase is also reactive in 1 M HCl (16 h), whereas the reduced Mo(IV)-S phase(s) in euxinic sediments, if associated with Fe-sulfides and/or organic matter, probably requires oxidative leaching with HNO_3 (Huerta-Diaz and Morse, 1992; Dahl et al., 2013). 3) The manganiferous Mo rich-deposits have only been observed in the abyssal ocean during slow deposition, while euxinic deposits can be found on the shelves where organic carbon sequestration is high.

More complex Mo concentration mechanisms exist in low oxygen, low sulfide settings, such as the pelagic zone of the Black Sea (Scholz et al., 2013). Mo is adsorbed onto Mn-(oxyhydr)oxides in oxic waters and will sink to the sulfidic bottom waters or sediments. In anoxic sediments Mn-oxide is removed during reductive dissolution, and lost to the water column, while Mo can be trapped in Mo-sulfides in the deeper sulfidic sedimentary layers. One possible example is Gullmar fjord,

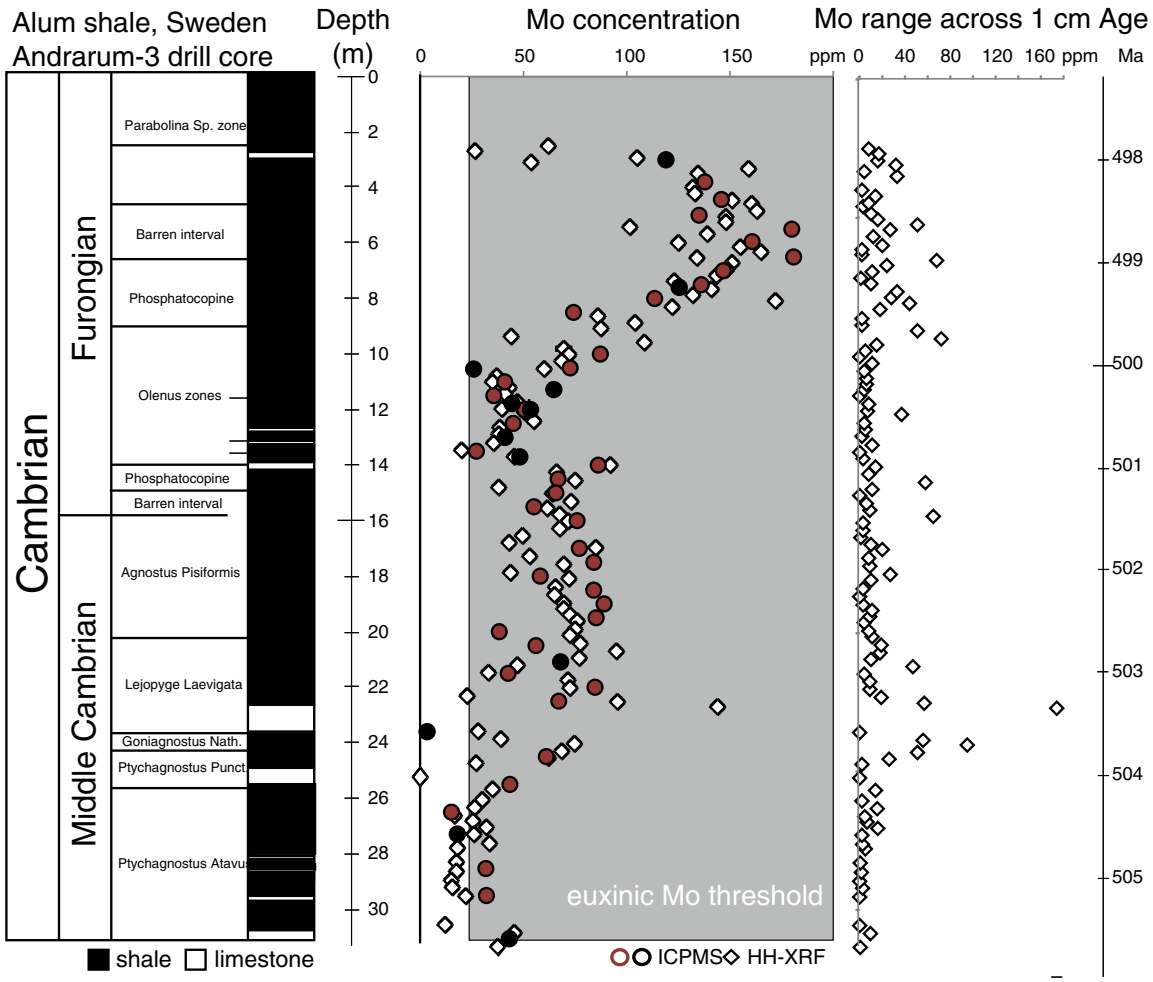

Fig. 4. Mo concentrations in Andrarum-3 drill core samples. Handheld XRF data (◊) is obtained directly on bedding planes compares to bulk rock data obtained using mass spectrometry (red, ▪, Gill et al., 2011; black ●, Dahl et al., 2010b). The Mo concentration difference between two stratigraphic intervals ~1 cm apart is plotted in the right panel. Biostratigraphy after (Ahlberg et al., 2009), chronostratigraphy is inferred by interpolation of the Cambrian series (Gradstein et al., 2008). (For interpretation of the references to color in this figure legend, the reader is referred to the web version of this article.)

Sweden (Goldberg et al., 2012). Here, Mo enrichments are, however, modest (~5 ppm) and our database likely contains no example of a setting that produces a false euxinic, >25 ppm Mo signal. Mo transport with Mn (oxyhydr)oxides through the oxic water column might be distinguished from Mo–Mn co-variation in the sediments, which is also observed in many oxic settings (e.g., Siebert et al., 2003; Chappaz et al., 2008). Thus, an elevated sedimentary Mo content shows that unless Mn-oxides are preserved, sulfide levels were high enough in the pore fluids or overlying water-column, for the Mo-oxide phase to convert to the diagenetically stable Mo-sulfides. Finally, we note that sediments deposited near Mo-rich sources may display a false-positive euxinic Mo enrichment signal. Since hydrothermal fluids are a source of Mo to the oceans (Wheat et al., 2002), these may induce Mo enrichment in nearby sediments. This caveat may potentially compromise paleoenvironmental interpretation, even though this database doesn't show any example hereof.

5.2. Interpretation of ancient sedimentary rocks

The comparative study of modern settings provides a basis for inferring the presence of sulfide in ancient basins with sedimentary Mo enrichments. Yet, we stress that there are important limitations to this approach. Although all necessary requirements for euxinic Mo removal exist today, required conditions may have differed in the past, including oceanic molybdenum availability, pH, FeS, organic matter and S^0 (e.g., Tribovillard et al., 2004; Vorlicek et al., 2004; Helz et al., 2011; Dahl et al., 2013). Theoretical and experimental studies show that seawater Mo inventory has increased over time in concert with oceans transiting into a more oxygenated state (Tribovillard et al., 2006; Scott et al., 2008; Dahl et al., 2010b, 2011). Prior to the Great Oxidation Event (~2.3 Ga) oceans probably contained <5% of today's level (Anbar et al., 2007; Scott et al., 2008; ~7 μM total sulfide, calculation in appendix of Wille et al., 2007). Only after the last major oxygenation episode in the Devonian, oceans might have contained Mo concentrations similar to today (Dahl et al., 2010b). Furthermore, basinal restriction may also cause Mo depletion in local areas of the ocean and reduce the degree of sedimentary Mo enrichment (Algeo and Lyons, 2006; McArthur et al., 2008). Unless Earth's oceans have experienced extreme Mo levels during some past times, we conclude that finding ancient organic-rich sediments with >25 ppm Mo concentrations is still a strong indication of deposition in euxinic, or at least intermittently euxinic, environments.

5.3. Comparison to other proxies for ocean euxinia

Other available indicators for water column euxinia include iron speciation data, Mo stable isotope compositions, pyrite framboid size distributions, and organic biomarkers. The iron speciation proxy can tell whether or not Fe^{2+} was mobilized in an anoxic basin and if sulfide concentrations were high enough to ultimately fix Fe in the form of

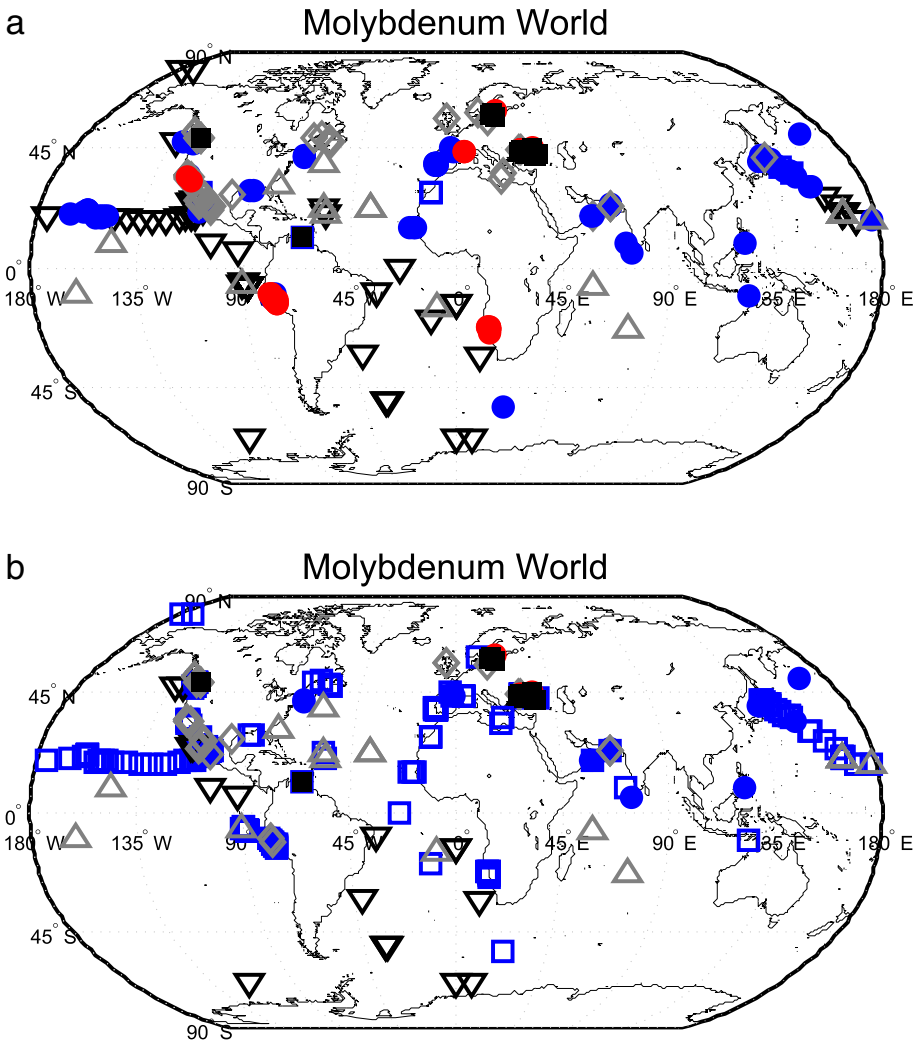

Fig. 5. a) Geographical distribution of 314 marine depositional sites with sedimentary Mo concentration profiles. In 172 cases, the Mo data is reported without measurements of the water column and sediment redox conditions, so redox conditions have been inferred based on comparison with other studies. b) At the other 136 sites the redox environments were independently determined with O_2 and H_2S data (▫). See Table 3 for legends and a statistical overview.

pyrite (Poulton and Canfield, 2005). Yet, the sulfide concentration for FeS formation (and subsequent pyrite formation in sediment) is even lower (>7 μM) than for efficient Mo scavenging (15–125 μM). Mo isotopes can provide evidence for low sulfide levels, since net isotope fractionation will be expressed in the sediments relative to overlying seawater, when there is inadequate sulfide or time available for quantitative molybdate conversion to reactive thiomolybdate speciation (Neubert et al., 2008; Dahl et al., 2010a; Nägler et al., 2011; Arnold et al., 2012). Small pyrite framboids with narrow size distributions are characteristic of pyrite formation in euxinic waters contrasting broader size spectrum in pyrites formed inside sulfidic sediments underlying oxic water (Wilkin et al., 1996). This may require a thicker sulfidic water column than for Mo enrichments. Additionally, Photic Zone Euxinia (PZE) can be preserved in the sediments as carotenoid pigments from anoxic photosynthetic bacteria, including isorenieratene (green sulfur bacteria) and carotenoid okenone (purple sulfur bacteria) (Brocks et al., 2005). Clearly, these biomarker signatures imply the presence of sulfide in the shallow photic zone. Of all these methods, the Mo-based euxinia proxy is now the easiest and most affordable analyses, applicable for large sample sets.

The various methods provide assisting characterizations of euxinic basins that, together, can be used to make firm conclusions, and perhaps even constrain the persistence of euxinia or estimate the thickness of the euxinic zone. We note that the Mo-proxy indicates euxinia also when sulfide is only intermittently present (e.g. Namibia and East Pacific). Although the Mo enrichments suggest euxinia in an ancient rock record, additional information is still required to infer the extent of euxinic water masses.

The Mo-based proxy has the advantage over chemical speciations, mineral structure and molecular tracers, because bulk Mo content is unchanged during early diagenesis (Dahl et al., 2013; Wirth et al., 2013), and presumably Mo is neither added nor lost during low grade metamorphism, though hydrothermal fluids flow are an exception that may circulate Mo through the rock and deposit Mo in the presence of sulfide.

6. Concluding remark

We conclude that handheld XRF enables precise and accurate Mo concentration determination in sedimentary rocks useful for field-based characterization of ancient euxinic environments. In fact, the Mo sensitivity of the HHXRF is significantly better than previous measurements using energy-dispersive polarization XRF applied on board an ODP research vessel (Wien et al., 2005). Finally, the technique has advantages over traditional mass spectrometry in several respects: It requires no sample preparation, it is easy to use, and it is portable in the field. For these reasons, HHXRF allows for high-resolution paleo-redox studies at much greater lateral and temporal resolution than ever before —

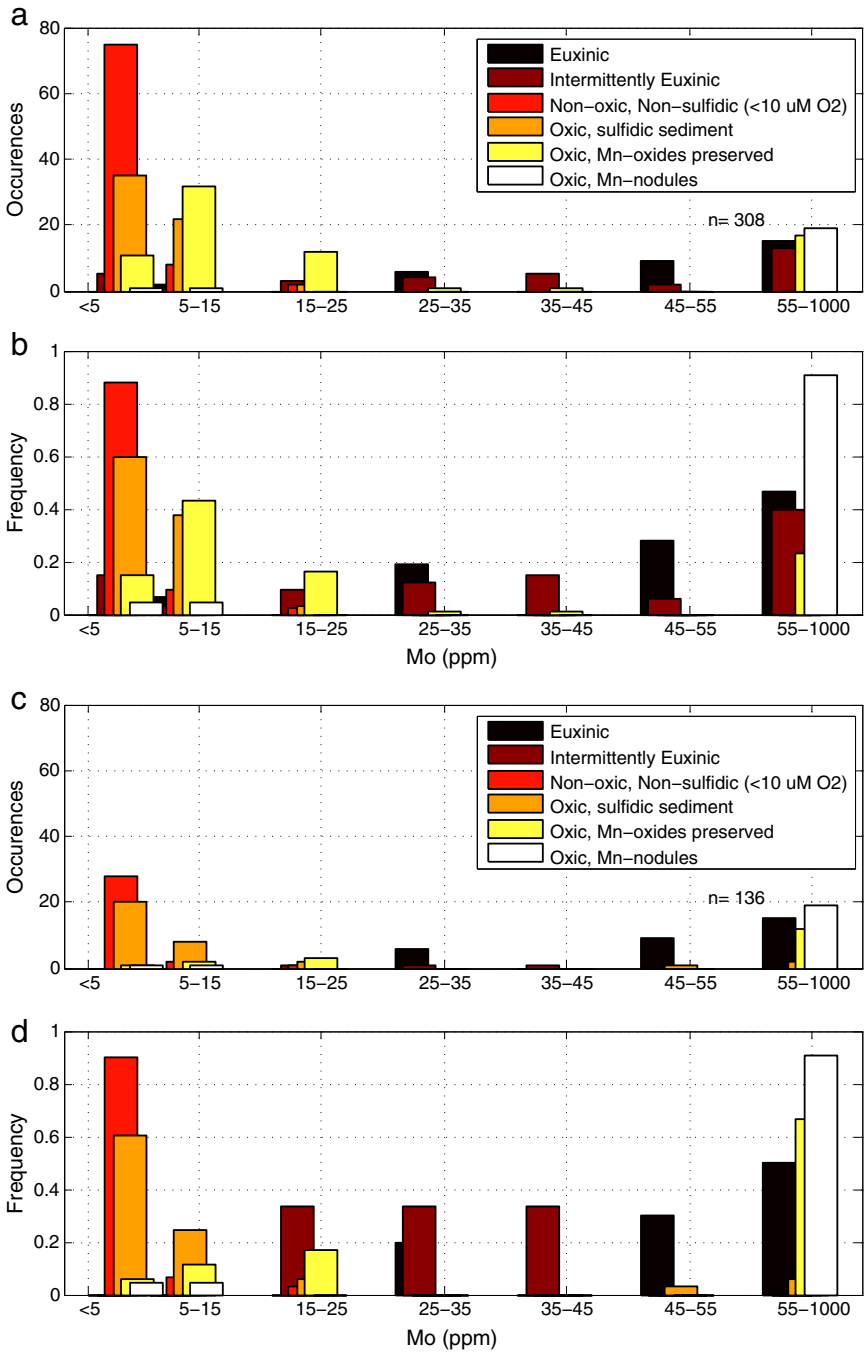

Fig. 6. a) Histogram and b) frequency of molybdenum concentrations of surface sediments for each redox category defined in Table 3. Strong Mo enrichments relative to average upper continental crust [~1.5 ppm,] and riverine particulates [~3 ppm,] occur in euxinic sediments deposited under a sulfidic water column and in Mn-oxide deposits. Mn-oxide rich sediments deposited slowly in the abyssal ocean at >3.5 km depth also yield > 25 ppm Mo (Table S2) with Mn-nodules extremely enriched at up to 700 ppm Mo. Panel c and d) are equivalent to a) and b), and show only the 172 sediment cores where redox conditions have been reported with the Mo data (see data and details in Table S2).

even in remote field sites or, perhaps, onboard robotic missions to our neighboring planets.

Supplementary data to this article can be found online at http://dx.doi.org/10.1016/j.chemgeo.2013.10.022.

Acknowledgments

First, we thank Bo Thamdrup for fruitful discussions. Thomas Sauer at Innov-X assisted us in the technical aspects of the instrument. The authors declare no financial interests in this work. A. Knoll financed some of the ICPMS analyses (NSF grant EAR-0420592) at Langmuir lab at Harvard University. Lab manager Z. Chen (Harvard) and J. Kystol (GEUS) assisted with ICPMS analyses. Funding was provided from Nordic Center for Earth Evolution (NordCEE) of the Danish National Research Foundation (Danmarks Grundforskningsfond, grant number DNRF53), and through Danish National Research Council (TWD: FNU 09-065813, CJB: FNU 09-064121), Villum Kann Rasmussen Foundation to TWD (ID: 1168439 and Young Investigator Grant VKR023127), Center for Macroecology, Evolution and Climate (MTR, TWD), the Dutch Niels Stensen Foundation (MR) and the Carlsberg Foundation (CJB and MR: 2011_01_0705).

Table 3
Overview of the sediment cores with Mo concentration data listed in Table S2.

Redox assignment[a]	Water column redox[b]	Sediment redox[c]	Expected delivery and capture process[d]	Expected Mo phase[e]	Realistic[f]	Strict[g]	Symbol infig. 1-2
Dysoxic	Oxic	Non-oxic, non-sulfidic	Mn-Ox delivery, reductive dissolution, little or no capture	none	85	31	●
Oxic	Oxic	Oxic	Mn-(and Fe-) oxide precipitation, preserved in nodules in the deep ocean	Mo-oxide in Mn nodules	21	21	△
Oxic	Oxic	Oxic	Mn-(and Fe-) oxide precipitation preserved in oxic sediments	Mo-oxide in Mn-oxides	74	18	▼
Sulfidic at depth	Oxic	Sulfidic	Mn-(and Fe-) Ox delivery, reductive dissolution, Mo capture in sulfidic zone	Mo-sulfide	4	0	◇
Sulfidic at depth	Non-oxic non-sulfidic	Sulfidic	dead organic matter and/or FeS and/or FeS2	Mo-sulfide	59	33	◇
Intermittently euxinic	Non-oxic/ intermittently sulfidic	Sulfidic	dead organic matter and/or FeS and/or FeS2	Mo-sulfide	33	3	●
Euxinic	Sulfidic	Sulfidic	dead organic matter and/or FeS and/or FeS2	Mo-sulfide	32	30	■
Unassigned	Unassigned	Unassigned	Unassigned	Unassigned	6	178	□
Total					314	314	

[a] The oxic and sulfidic thresholds are defined at >10 μM O2 and >10 μM H2S, where Mn-oxides can persist and thiomolybdates will form, respectively (Shaw et al., 1990; Helz et al., 1996).
[b] The water column redox represents near bottom water redox conditions.
[c] Sediment redox is the redox composition observed within the measured depths of the sediment.
[d] Inferred Mo delivery and capture process.
[e] Expected terminal Mo speciation are listed.
[f] The strict redox categorization is based on reported O2 and H2S profiles with the Mo data.
[g] The realistic categorization is based O2 and H2S reported in other work. The presence of Mn-nodules is taken as an independent evidence for oxic conditions. All reported data are summarized in Table S2.

References

Ahlberg, P.E.R., Axheimer, N., Babcock, L.E., Eriksson, M.E., Schmitz, B., Terfelt, F., 2009. Cambrian high-resolution biostratigraphy and carbon isotope chemostratigraphy in Scania, Sweden: first record of the SPICE and DICE excursions in Scandinavia. Lethaia 42, 2–16.

Algeo, T.J., Lyons, T.W., 2006. Mo-total organic carbon covariation in modern anoxic marine environments: Implications for analysis of paleoredox and paleohydrographic conditions. Paleoceanography 21, 1–23.

Anbar, A.D., 2004. Molybdenum stable isotopes: observations, interpretations and directions. Rev. Mineral. Geochem. 55, 429–454.

Anbar, A.D., Duan, Y., Lyons, T.W., Arnold, G.L., Kendall, B., Creaser, R.A., Kaufman, A.J., Gordon, G.W., Scott, C., Garvin, J., Buick, R., 2007. A whiff of oxygen before the great oxidation event? Science 317, 1903–1906.

Arnold, G.L., Lyons, T.W., Gordon, G.W., Anbar, A.D., 2012. Extreme change in sulfide concentrations in the Black Sea during the Little Ice Age reconstructed using molybdenum isotopes. Geology 40, 595–598.

Bender, M.L., Heggie, D.T., 1984. Fate of organic carbon reaching the deep sea floor: a status report. Geochim. Cosmochim. Acta 48, 977–986.

Bertine, K., Turekian, K., 1973. Molybdenum in marine deposits. Geochim. Cosmochim. Acta 37, 1415–1434.

Böning, P., Brumsack, H.-J., Böttcher, M.E., Schnetger, B., Kriete, C., Kallmeyer, J., Borchers, S.L., 2004. Geochemistry of Peruvian near-surface sediments. Geochim. Cosmochim. Acta 68, 4429–4451.

Bostick, B.C., Fendorf, S., Helz, G.R., 2003. Differential adsorption of molybdate and tetrathiomolybdate on pyrite (FeS2). Environ. Sci. Technol. 37, 285–291.

Brocks, J.J., Love, G.D., Summons, R.E., Knoll, A.H., Logan, G.A., Bowden, S.A., 2005. Biomarker evidence for green and purple sulphur bacteria in a stratified Palaeoproterozoic sea. Nature 437, 866–870.

Brongersma-Sanders, M., Stephan, K.M., Kwee, T.G., De Bruin, M., 1980. Distribution of minor elements in cores from the Southwest Africa shelf with notes on plankton and fish mortality. Mar. Geol. 37, 91–132.

Brucker, R.L.P., McManus, J., Severmann, S., Berelson, W.M., 2009. Molybdenum behavior during early diagenesis: Insights from Mo isotopes. Geochem. Geophys. Geosyst. 10, 25.

Calvert, S.E., Pedersen, T.F., 1993. Geochemistry of Recent oxic and anoxic marine sediments: Implications for the geological record. Mar. Geol. 113, 67–88.

Canfield, D., 2005. The early history of atmospheric oxygen: Homage to Robert M Garrels. Annu. Rev. Earth Planet. Sci. 33, 1–36.

Chaillou, G., Anschutz, P., Lavaux, G., Schafer, J., Blanc, G., 2002. The distribution of Mo, U, and Cd in relation to major redox species in muddy sediments of the Bay of Biscay. Mar. Chem. 80, 41–59.

Chappaz, A., Gobeil, C., Tessier, A., 2008. Geochemical and anthropogenic enrichments of Mo in sediments from perennially oxic and seasonally anoxic lakes in Eastern Canada. Geochim. Cosmochim. Acta 72, 170–184.

Dahl, T.W., Anbar, A.D., Gordon, G.W., Rosing, M.T., Frei, R., Canfield, D.E., 2010a. The behavior of molybdenum and its isotopes across the chemocline and in the sediments of sulfidic Lake Cadagno, Switzerland. Geochim. Cosmochim. Acta 74, 144–163.

Dahl, T.W., Hammarlund, E.U., Anbar, A.D., Bond, D.P.G., Gill, B.C., Gordon, G.W., Knoll, A.H., Nielsen, A.T., Schovsbo, N.H., Canfield, D.E., 2010b. Devonian rise in atmospheric oxygen correlated to the radiations of terrestrial plants and large predatory fish. Proc. Natl. Acad. Sci. 107, 17911–17915.

Dahl, T.W., Canfield, D.E., Rosing, M.T., Frei, R.E., Gordon, G.W., Knoll, A.H., Anbar, A.D., 2011. Molybdenum evidence for expansive sulfidic water masses in 750 Ma oceans. Earth Planet. Sci. Lett. 311, 264–274.

Dahl, T.W., Chappaz, A., Fitts, J.P., Lyons, T.W., 2013. Molybdenum reduction in a sulfidic lake: evidence from X-ray absorption fine-structure spectroscopy and implications for the Mo paleoproxy. Geochim. Cosmochim. Acta 103, 213–231.

Emerson, S., Huested, S.S., 1991. Ocean anoxia and the concentrations of molybdenum and vanadium in seawater. Mar. Chem. 34, 177–196.

Erickson, B.E., Helz, G.R., 2000. Molybdenum(VI) speciation in sulfidic waters: stability and lability of thiomolybdates. Geochim. Cosmochim. Acta 64, 1149–1158.

Fang, L., Bjerrum, C.J., Hesselbo, S.P., Kotthoff, U., McCarthy, F.M.G., Huang, B., Ditchfield, P.W., 2013. Carbon-isotope stratigraphy from terrestrial organic matter through the Monterey event, Miocene, New Jersey margin (IODP Expedition 313). Geosphere 9, 1–16.

Farquhar, J., Bao, H.M., Thiemens, M., 2000. Atmospheric influence of Earth's earliest sulfur cycle. Science 289, 756–758.

Gill, B.C., Lyons, T.W., Young, S.A., Kump, L.R., Knoll, A.H., Saltzman, M.R., 2011. Geochemical evidence for widespread euxinia in the later Cambrian ocean. Nature 469, 80–83.

Goldberg, T., Archer, C., Vance, D., Thamdrup, B., McAnena, A., Poulton, S.W., 2012. Controls on Mo isotope fractionations in a Mn-rich anoxic marine sediment, Gullmar Fjord, Sweden. Chem. Geol. 296–297, 73–82.

Govindaraju, K., 1994. 1994 Compilation of Working Values and Sample Description for 383 Geostandards. Geostand. Newslett. 18, 1–158.

Gradstein, F.M., Ogg, J.G., van Kranendonk, M., 2008. On the geologic time scale 2008. Newsl. Stratigr. 43, 5–13.

Hammarlund, E.U., Dahl, T.W., Harper, D.A.T., Bond, D.P.G., Nielsen, A.T., Bjerrum, C.J., Schovsbo, N.H., Schönlaub, H.P., Zalasiewicz, J.A., Canfield, D.E., 2012. A sulfidic driver for the end-Ordovician mass extinction. Earth Planet. Sci. Lett. 331–332, 128–139.

Helz, G.R., Miller, C.V., Charnock, J.M., Mosselmans, J.F.W., Pattrick, R.A.D., Garner, C.D., Vaughan, D.J., 1996. Mechanism of molybdenum removal from the sea and its concentration in black shales: EXAFS evidence. Geochim. Cosmochim. Acta 60, 3631–3642.

Helz, G.R., Vorlicek, T.P., Kahn, M.D., 2004. Molybdenum scavenging by iron monosulfide. Environ. Sci. Technol. 38, 4263–4268.
Helz, G.R., Bura-Nakić, E., Mikac, N., Ciglenečki, I., 2011. New model for molybdenum behavior in euxinic waters. Chem. Geol. 284, 323–332.
Hershey, J.P., Plese, T., Millero, F.J., 1988. The pK1* for the dissociation of H2S in various ionic media. Geochim. Cosmochim. Acta 52, 2047–2051.
Holland, H.D., 1984. The Chemical Evolution of the Atmosphere and Oceans. Princeton University Press.
Holland, H.D., 2006. The oxygenation of the atmosphere and oceans. Philos. Trans. R. Soc. Lond. B Biol. Sci. 361, 903–915.
Huerta-Diaz, M.A., Morse, J.W., 1992. Pyritization of trace metals in anoxic marine sediments. Geochim. Cosmochim. Acta 56, 2681–2702.
Isozaki, Y., 1997. Permo-Triassic boundary superanoxia and stratified superocean: records from lost deep sea. Science 276, 235–238.
Jaraula, C.M.B., Grice, K., Twitchett, R.J., Bottcher, M.E., LeMetayer, P., Dastidar, A.G., Opazo, L.F., 2013. Elevated pCO2 leading to Late Triassic extinction, persistent photic zone euxinia, and rising sea levels. Geology 41, 955–958.
Jenkyns, H.C., 2010. Geochemistry of oceanic anoxic events. Geochem. Geophys. Geosyst. 11, 1–30.
Knoll, A.H., Bambach, R.K., Canfield, D.E., Grotzinger, J.P., 1996. Comparative earth history and Late Permian mass extinction. Science 273, 452–457.
Lauridsen, B.W., Nielsen, A.T., 2005. The Upper Cambrian Trilobite Olenus at Andrarum, Sweden: a case of iterative evolution? Palaeontology 48, 1041–1056.
Lavik, G., Stuhrmann, T., Bruchert, V., Van der Plas, A., Mohrholz, V., Lam, P., Mussmann, M., Fuchs, B.M., Amann, R., Lass, U., Kuypers, M.M., 2009. Detoxification of sulphidic African shelf waters by blooming chemolithotrophs. Nature 457, 581–584.
Lyons, T.W., Anbar, A.D., Severmann, S., Scott, C., Gill, B.C., 2009. Tracking euxinia in the ancient ocean: a multiproxy perspective and proterozoic case study. Annu. Rev. Earth Planet. Sci. 37, 507–534.
Macquaker, J.H.S., Keller, M.A., Davies, S.J., 2010. Algal blooms and "marine snow": mechanisms that enhance preservation of organic carbon in ancient fine-grained sediments. J. Sediment. Res. 80, 934–942.
Malcolm, S., 1985. Early diagenesis of molybdenum in estuarine sediments. Mar. Chem. 16, 213–225.
Mao, X., Hou, X., Li, C., Ouyang, H., Chai, Z., 2001. Determination of platinum-group elements and forty two other elements in two candidate Danish Cretaceous–Tertiary boundary clay reference materials by INAA, ENAA and RNAA. Geostand. Newslett. 25, 167–171.
McArthur, J.M., Algeo, T.J., van de Schootbrugge, B., Li, Q., Howarth, R.J., 2008. Basinal restriction, black shales, Re–Os dating, and the Early Toarcian (Jurassic) oceanic anoxic event. Paleoceanography 23, 1–22.
Meyer, K.M., Kump, L.R., 2008. Oceanic euxinia in earth history: causes and consequences. Annu. Rev. Earth Planet. Sci. 36, 251–288.
Morford, J.L., Emerson, S., 1999. The geochemistry of redox sensitive trace metals in sediments. Geochim. Cosmochim. Acta 63, 1735–1750.
Morford, J.L., Emerson, S.R., Breckel, E.J., Kim, S.H., 2005. Diagenesis of oxyanions (V, U, Re, and Mo) in pore waters and sediments from a continental margin. Geochim. Cosmochim. Acta 69, 5021–5032.
Moseley, H.G.J., 1913. The high-frequency spectra of the elements. Philos. Mag. 26, 1024–1034.
Mountain, G., Proust, J.-N., McInroy, D., Cotterill, C., Expedition-313-Scientists, 2010. Proc. IODP, 313. Integrated Ocean Drilling Program Management International, Inc., Tokyo, p. 450. http://dx.doi.org/10.2204/iodp.proc.313.2010.
Nägler, T.F., Neubert, N., Böttcher, M.E., Dellwig, O., Schnetger, B., 2011. Molybdenum isotope fractionation in pelagic euxinia: evidence from the modern Black and Baltic Seas. Chem. Geol. 289, 1–11.
Neubert, N., Nägler, T.F., Böttcher, M.E., 2008. Sulfidity controls molybdenum isotope fractionation into euxinic sediments: evidence from the modern Black Sea. Geology 36, 775–778.
Pattan, J.N., Pearce, N.J.G., 2009. Bottom water oxygenation history in southeastern Arabian Sea during the past 140 ka: Results from redox-sensitive elements. Palaeogeogr. Palaeoclimatol. Palaeoecol. 280, 396–405.
Piper, D.Z., Calvert, S.E., 2011. Holocene and late glacial palaeoceanography and palaeolimnology of the Black Sea: changing sediment provenance and basin hydrography over the past 20,000 years. Geochim. Cosmochim. Acta 75, 5597–5624.
Poulton, S., Canfield, D., 2005. Development of a sequential extraction procedure for iron: implications for iron partitioning in continentally derived particulates. Chem. Geol. 214, 209–221.
Poulton, S.W., Fralick, P.W., Canfield, D.E., 2004. The transition to a sulphidic ocean similar to 1.84 billion years ago. Nature 431, 173–177.
Rowe, H., Hughes, N., Robinson, K., 2012. The quantification and application of handheld energy-dispersive X-ray fluorescence (ED-XRF) in mudrock chemostratigraphy and geochemistry. Chem. Geol. 324–325, 122–131.
Ruhl, M., Kürschner, W.M., Krystyn, L., 2009. Triassic–Jurassic organic carbon isotope stratigraphy of key sections in the western Tethys realm (Austria). Earth Planet. Sci. Lett. 281, 169–187.
Schlanger, S.O., Jenkyns, H.C., 1976. Cretaceous oceanic anoxic events: causes and consequences. Geol. Mijnb. 55, 179–184.
Schnetger, B., 1997. Trace element analysis of sediments by HR-ICP-MS using low and medium resolution and different acid digestions. Fresenius J. Anal. Chem. 359, 468–472.
Scholz, F., McManus, J., Sommer, S., 2013. The manganese and iron shuttle in a modern euxinic basin and implications for molybdenum cycling at euxinic ocean margins. Chem. Geol. 355, 56–68.
Schunck, H., Lavik, G., Desai, D.K., Großkopf, T., Kalvelage, T., Löscher, C.R., Paulmier, A., Contreras, S., Siegel, H., Holtappels, M., Rosenstiel, P., Schilhabel, M.B., Graco, M., Schmitz, R.A., Kuypers, M.M.M., LaRoche, J., 2013. Giant hydrogen sulfide plume in the oxygen minimum zone off Peru supports chemolithoautotrophy. PLoS ONE 8, e68661.
Scott, C., Lyons, T.W., 2012. Contrasting molybdenum cycling and isotopic properties in euxinic versus non-euxinic sediments and sedimentary rocks: refining the paleoproxies. Chem. Geol. 324–325, 19–27.
Scott, C., Lyons, T.W., Bekker, A., Shen, Y., Poulton, S.W., Chu, X., Anbar, A.D., 2008. Tracing the stepwise oxygenation of the Proterozoic ocean. Nature 452, 456–459.
Shaw, T.J., Gieskes, J.M., Jahnke, R.A., 1990. Early diagenesis in differing depositional environments: the response of transition metals in pore water. Geochim. Cosmochim. Acta 54, 1233–1246.
Shimmield, G., Price, N., 1986. The behaviour of molybdenum and manganese during early sediment diagenesis offshore Baja California, Mexico. Mar. Chem. 19, 261–280.
Siebert, C., Nägler, T.F., von Blanckenburg, F., Kramers, J.D., 2003. Molybdenum isotope records as a potential new proxy for paleoceanography. Earth Planet. Sci. Lett. 211, 159–171.
Tribovillard, N., Riboulleau, A., Lyons, T., Baudin, F., 2004. Enhanced trapping of molybdenum by sulfurized marine organic matter of marine origin in Mesozoic limestones and shales. Chem. Geol. 213, 385–401.
Tribovillard, N., Algeo, T.J., Lyons, T., Riboulleau, A., 2006. Trace metals as paleoredox and paleoproductivity proxies: an update. Chem. Geol. 232, 12–32.
Vorlicek, T.P., Helz, G.R., 2002. Catalysis by mineral surfaces: implications for Mo geochemistry in anoxic environments. Geochim. Cosmochim. Acta 66, 3679–3692.
Vorlicek, T.P., Kahn, M.D., Kasuya, Y., Helz, G.R., 2004. Capture of molybdenum in pyrite-forming sediments: role of ligand-induced reduction by polysulfides. Geochim. Cosmochim. Acta 68, 547–556.
Wasylenki, L.E., Weeks, C.L., Bargar, J.R., Spiro, T.G., Hein, J.R., Anbar, A.D., 2011. The molecular mechanism of Mo isotope fractionation during adsorption to birnessite. Geochim. Cosmochim. Acta 75, 5019–5031.
Weeks, S.J., Currie, B., Bakun, A., Peard, K.R., 2004. Hydrogen sulphide eruptions in the Atlantic Ocean off southern Africa: implications of a new view based on SeaWiFS satellite imagery. Deep-Sea Res. I Oceanogr. Res. Pap. 51, 153–172.
Wheat, C.G., Mottl, M.J., Rudnicki, M., 2002. Trace element and REE composition of a low-temperature ridge-flank hydrothermal spring. Geochim. Cosmochim. Acta 66, 3693–3705.
Wien, K., Wissmann, D., Kölling, M., Schulz, H.D., 2005. Fast application of X-ray fluorescence spectrometry aboard ship: how good is the new portable Spectro Xepos analyser? Geo-Mar. Lett. 25, 248–264.
Wilkin, R.T., Barnes, H.L., Brantley, S.L., 1996. The size distribution of framboidal pyrite in modern sediments: an indicator of redox conditions. Geochim. Cosmochim. Acta 60, 3897–3912.
Wille, M., Kramers, J.D., Nagler, T.F., Beukes, N.J., Schroder, S., Meisel, T., Lacassie, J.P., Voegelin, A.R., 2007. Evidence for a gradual rise of oxygen between 2.6 and 2.5 Ga from Mo isotopes and Re-PGE signatures in shales. Geochimica Et Cosmochimica Acta 71, 2417–2435.
Wirth, S.B., Gilli, A., Niemann, H., Dahl, T.W., Ravasi, D., Sax, N., Hamann, Y., Peduzzi, R., Peduzzi, S., Tonolla, M., Lehmann, M.F., Anselmetti, F.S., 2013. Combining sedimentological, trace metal (Mn, Mo) and molecular evidence for reconstructing past water-column redox conditions: the example of meromictic Lake Cadagno (Swiss Alps). Geochim. Cosmochim. Acta 120, 220–238.
Zheng, Y., Anderson, F., 2000. Authigenic molybdenum formation in marine sediments: a link to pore water sulfide in the Santa Barbara Basin. Geochim. Cosmochim. Acta 64, 4165–4178.